Impact Assessment on Aerospace Structures

BTP Report

by

AUGUSTA BHARADWAJ AND HARSH YADAV
Roll. No. 200103025 and 200103049

Under Prof. Niranjan Sahoo

Department of Mechanical Engineering
Indian Institute of Technology Guwahati
Guwahati – 781039, Assam, India
April ,2024

Acknowledgement

Firstly, we owe our very heartfelt gratitude and deepest regard to my supervisor, Professor Niranjan Sahoo, Department of Mechanical Engineering, IIT Guwahati, India, for his relentless guidance, constant support and full cooperation throughout the project. His methods, vision and enthusiasm has always been a constant motivation and inspiration to me. Without his supervision and direction, this project could not have been a success.

We would also like to express our gratitude to our guide Mr. Amit, PhD scholar Department of Mechanical Engineering, IIT Guwahati, India, who has always guided us all the way through this phase of BTP and helped us get through every problem we faced during this time.

Augusta Bharadwaj and Harsh Yadav
April 24,2024

Abstract

This study delves into the mechanical properties and behavior of hybrid aluminum metal matrix composite foams under different loading scenarios, with a focus on their application in aerospace engineering. Comprising LM-13 aluminum alloy enhanced with 3% Boron Carbide (B4C) and 0.5% graphene nanoparticles by weight, the composites are evaluated for their performance under quasi-static uniaxial compressive loading and dynamic high-strain shock loadings. The analysis includes the compressive strength, energy absorption capabilities, stress-strain characteristics, and deformation behavior under impact conditions.

Our findings reveal that the integration of boron carbide and graphene nanoparticles significantly bolsters the mechanical attributes of the aluminum foams, resulting in enhanced structural robustness and lower density. These improvements contribute to superior energy absorption and heightened resistance to dynamic impacts, which are crucial for aerospace structures. Additionally, theoretical calculations and ABAQUS CAE simulations provide comprehensive insights into the impact resistance and structural integrity, illustrating the potential of these materials in augmenting the safety and durability of aerospace structures against abrupt energetic impacts.

This project paves the way for future explorations into optimizing composite formulas and refining manufacturing techniques to maximize aerospace application performance. Upcoming research efforts will assess the scalability of production methods and explore the long-term resilience of the composite material under various environmental stressors. By advancing our understanding of metal foam composites, this study highlights their promising potential in vital applications where exceptional energy absorption and mechanical strength are essential.

Contents

Nomenclature

Latin Symbols

Al	Aluminium
BaH_2	Barium Hydroxide
$CaCO_3$	Calcium Carbonate
E	Young's Modulus
L	Length (m)
m	Strain rate sensitivity
Mg	Magnesium
P	Pressure (Pa)
T	Temperature (K)
TiH_2	Titanium Hydroxide
W_s	Wave speed
Zn	Zinc

Abbreviations

Alcan	Aluminium Company of Canada
BRL	Bjorksten Research Laboratory
EDM	Electrical Discharge Machining

Literature Review

The use of metal foams in engineering applications, particularly in aerospace and automotive industries, has gained significant attention due to their unique properties such as low density, high energy absorption, and good thermal and acoustic insulation characteristics. This literature review synthesizes recent advancements in the development, characterization, and application of metal foams, with a special focus on aluminum metal matrix composites reinforced with nanoparticles.

The historical development of metal foams has been extensively documented in the literature. According to Banhart (2013), metal foams were initially conceptualized in the early 20th century, but significant advancements in manufacturing techniques have only been realized in recent decades. The introduction of gas-releasing particle decomposition methods and advanced alloying techniques has facilitated the production of metal foams with controlled porosity and enhanced mechanical properties (Fleck, 2016).

Several studies have explored the mechanical properties of metal foams under various loading conditions. Dannemann and Lankford (2000) investigated the high strain rate compression of closed-cell aluminum foams and highlighted their potential in impact mitigation applications due to their capacity to absorb significant energy while maintaining structural integrity. Recent research by Golestanipour et al. (2020) expanded on this by examining the perforation behavior of sandwich panels with composite foam cores, demonstrating improved resistance to high-velocity impacts.

The incorporation of nanoparticles such as graphene and boron carbide has been shown to further enhance the mechanical properties of aluminum foams. Research by An et al. (2017) revealed that graphene nanoparticles could significantly improve the tensile strength and impact resistance of aluminum foams by promoting more uniform stress distribution and crack resistance. Similarly, studies by Hou et al. (2010) have shown that boron carbide reinforcement leads to increased hardness and better wear resistance, making these composites more suitable for aerospace applications where high performance under extreme conditions is required.

Theoretical modeling and numerical simulations have become invaluable tools in predicting the behavior of metal foams under impact conditions. The use of finite element software like ABAQUS for simulating the dynamic response of foam structures has been detailed by authors such as Jing et al. (2017), who modeled the deformation and failure mechanisms of layered gradient metallic foam cores under ballistic impact

INTRODUCTION

1.1 Background

When there is a sudden input of energy it is in the form of impact. This creates very high strain rates, such that most of structures undergoing the impact are not be able to dissipate this impact energy, which in turn leads to failure of the structure. The energy might be produced due to a collision, blast or shock impacts. The failure of energy dissipation may cause big failures of Aerospace structures and also leads to severe casualties. Hence, it becomes very crucial to implement energy absorption property to the material which is being used to construct these structures which may have high probability to experience dynamic impacts. The material being used to absorb the energy plays a crucial role in the process of energy absorption, hence necessary precautions should be taken when designing and choosing this material. Our project is focused on the goal of coming up with an energy-absorbing material that can be used to protect objects from shock impacts where a sudden input of energy results in accidents and casualties, through the study and research of lightweight energy-absorbing materials.

1.2 Motivation of the study

A shock wave can be defined as a disturbance or a discontinuity that travels in medium which leads to major changes in properties such as pressure, temperature, velocity of a particle etc. A shock wave caused in aerospace / civil structures due to phenomena such as explosions or gunshots can result in severe accidents and casualties. Here comes the requirement of an energy absorbing material that can protect the object being humans, civil structures or automobiles from this shock impact. Therefore, to identify a suitable energy absorbing material to dissipate the shock impact during high strain rates situations can be of great use in such situations. Using these we can make buildings, aircrafts and automobiles hard enough to resist damage from such blasts. It is crucial to understand the impact behavior response for these materials under such critical impact loading conditions so as to develop and design a suitable impact resistance energy absorbing material. Studying the effect of different shock impact on metal

foams and produce experimental results .The mechanical, thermal and physical of this class of material feasible for wide range applications in aerospace and civil structures.

1.3 Metal Foams

Upon considering all the evident usefulness of metal foams, we started to study more about them and their making and properties.

Metal foams is a new class of material. They have low densities and novel physical, mechanical, thermal, electrical and acoustic properties. Which offer the potential for lightweight structures, energy absorption, and thermal management; at least, some are cheap.

Metallic foams also show significant performance gains in light, stiff structures that are highly efficient in energy absorption and thermal management.

During an impact, metallic foams deform, increasing the total time of energy dispersion and thus reducing the resulting forces on the body.

They are very light (low density) as compared to their respective metal alloys and the cost of production of metallic foam is also relatively low.

1.3.1 History of Metal Foams

A big proportion of innovations in the past were inspired from nature, Metal foams which are also known as “Metfoams” in (Fleck 2016) are one of its class inspired by material available in nature such as wood, pumice stone or bone. The idea of metal foam was first coined by the author De Meller (John Banhart 2013) in the year 1925. According to his patent, the process of making metal foam comprises of injection of inert gas into a molten metal or addition of a blowing agent such as a carbonate to a molten metal, during which the melt is stirred. He also mentioned ideas about production of integral foams by re-melting the surface of a metal foam, by immersing a foam into a molten metal bath or by centrifugal or pressing techniques that remove some liquid from a foam and form the outer cover layer. He has shown only a drawing of imagination but there is no mention of any originally produced object. Over the years there is a continuous development in the manufacturing techniques of these metal foams. Currently, we have many approaches for manufacturing metal foams based on required properties.

1.3.2 Making of metallic foams

1.3.2.1 Gas-releasing particle decomposition in the melt

The properties of the metal foam and other cellular metal structures depend upon the properties of the metal, the relative density and cell topology (e.g. open or closed cell, cell size, etc.).

There are a few distinct process routes, that have been developed to make metal foams in the industry, of which we will be looking into the process that we have chosen to adopt.

We have chosen LM-13 aluminum alloy for our research purpose, mixed with 0.5% graphene and 3% Boron carbide (B4C) by weight for reinforcement and strengthening the alloy.

The alloy will be foamed by mixing the metal into a foaming agent that releases gas when heated.

The process begins by melting aluminum and stabilizing the melt temperature between 670°C and 690°C. Its viscosity is then raised by adding 1–2% calcium, rapidly oxidizing and forming finely dispersed CaO and $CaAl_2O_4$ particles.

As soon as these are dispersed in the melt, the stirring system is withdrawn, and foam is allowed to form above the melt under a controlled environment by adjusting the pressure, temperature and time of foaming.

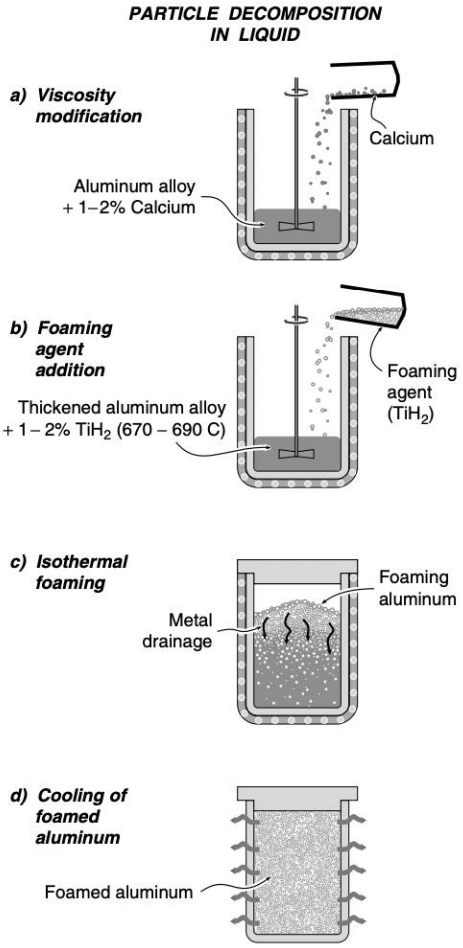

fig 1- The process steps used in the manufacture of aluminum foams by gas-releasing particle decomposition in the melt (Alporas process)

1.3.3 Properties of metal foams

The characteristics of foam are best summarized by describing the material from which it is made, additive substance, its relative density, and whether it has open or closed cells structure. Beyond this, foam properties are influenced by structure, mainly by anisotropy and by defects – by which we mean wiggly, buckled or broken cell walls and cells of exceptional size or shape.

In general metal foams are ultra-light materials with high porosity ,low thermal conductivity, great sound absorption and good compressive strength.

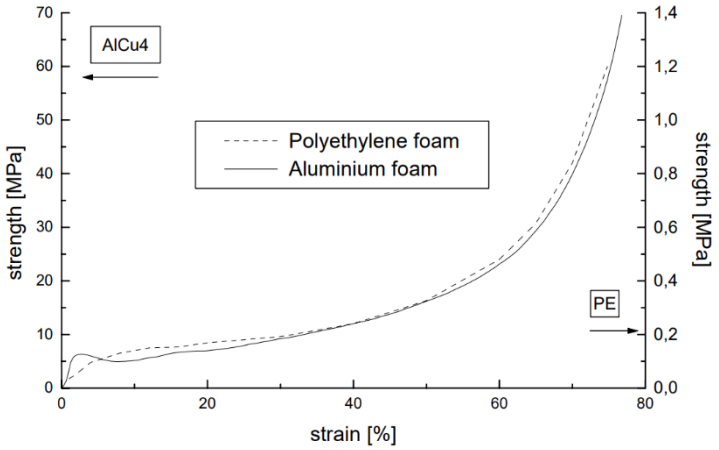

Figure 2 : Strength vs Strain curve of aluminum and polyethylene foams.

1.4 Foam structure

The characteristics of the foam structure are controlled mainly by particles in the metal matrix, viscosity, cooling rate, temperature of the melt and controlled injection of air/gas. Furthermore, continuous production of foam is required to achieve a particular foam density.

The structure of metal foams from three different suppliers: Cymat, Mepura (Alright) and Shinko (Alporas). The structures are like soap films: polyhedral cells with thin cell faces bordered by thicker cell edges ('Plateau borders'). Some features appear to be governed by surface energy, as in soap films: the Plateau borders are an example. But others are not: many faces have non-uniform curvature or are corrugated and have occasionally broken walls that still hang in place.

The three figures are ordered such that the relative density increases from the top to the bottom. And as it can be clearly observed that there is a difference in density, cell wall thickness, cell size and concentration.

Fig 3: Distinct types of foam structures

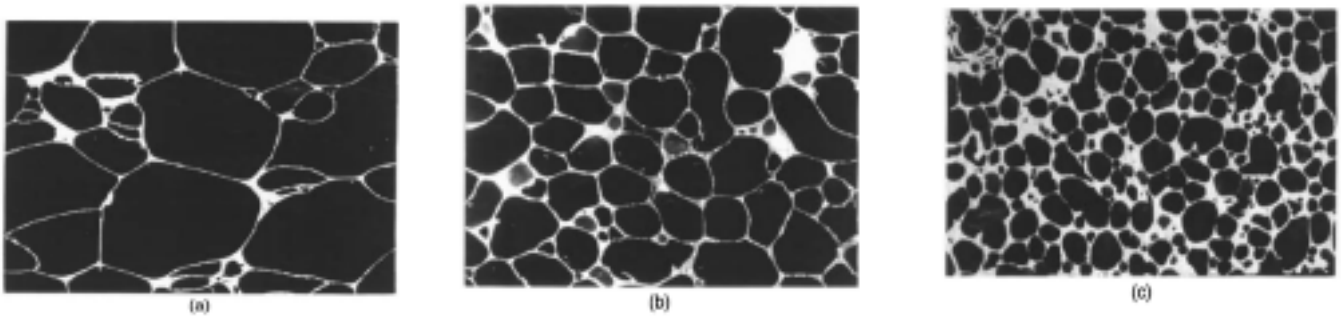

1.4.1 Open-cell metallic foam structure.

Open-cell foams are permeable materials with metallic properties. They feature a very homogeneous structure which guarantees constant characteristics over a wide range.

Open-cell metal foams can be produced in a large spectrum of pore sizes and densities. The adjustable pore sizes range from 0.3 to 5 mm, and the relative density can vary between 5 and 30 %. Because of the structure's high variability, functional properties like mechanical strength, sound absorption, and fluid and heat transfer can be precisely adjusted. With this, available materials with an enormous application range arise

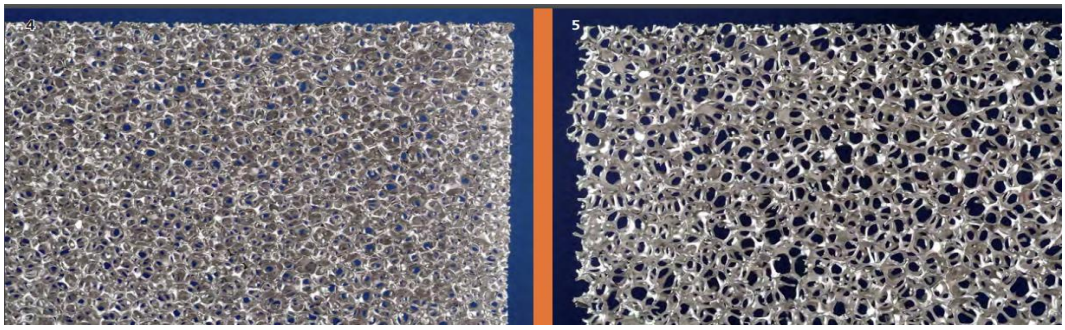

Figure 4: Open cell aluminum foam structures

1.4.2 Closed-cell metallic foam structure

Closed-cell metal foams are primarily used as an impact-absorbing material, similar to the polymer foams in a bicycle helmet but for higher impact loads. Unlike many polymer foams, metal foams remain deformed after impact and can only be deformed once. They are light (typically 10–25% of the density of an identical non-porous alloy, commonly those of aluminium) and stiff and are frequently proposed as a lightweight structural material. However, they have not been widely used for this purpose.

Closed-cell foams also add the property of flotation in water while retaining the fire resistance and recycling potential of other metal foams.

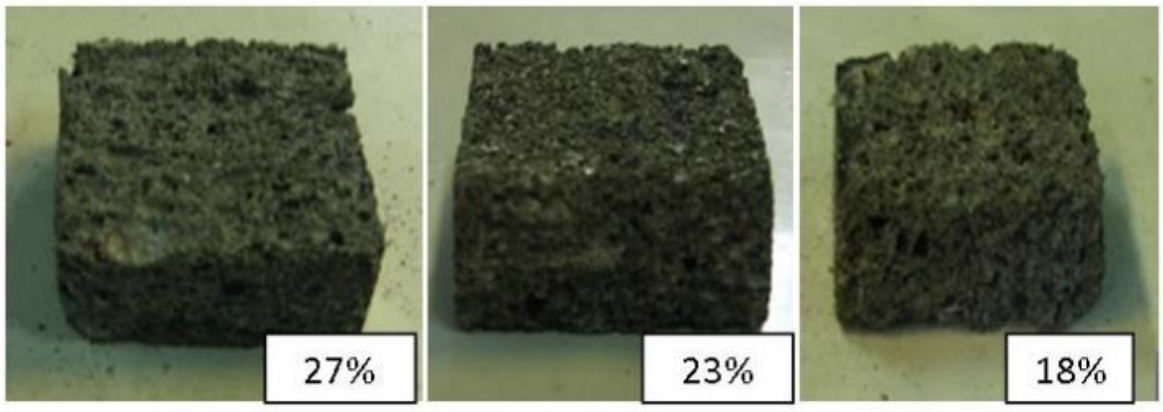

Figure 5: Closed cell aluminum foam structures

1.4.3 Aluminum Foam Sandwich

- One of the superior metal foams used by previous researchers in automotive applications is the aluminum foam sandwich due to its unique properties, such as low density and superior energy absorption characteristics
- Aluminium foam sandwich panels are good energy absorbers and lightweight, providing a wide range of applications in automotive industries.
- The sandwich panel structures with aluminium foam core and metal surfaces have lightweight with high performance in dispersing energy. This has led to their widespread use in the absorption of energy. The cell structure of the foam core is subjected to plastic deformation in the constant tension level that absorbs a lot of kinetic energy before the destruction of the structure.

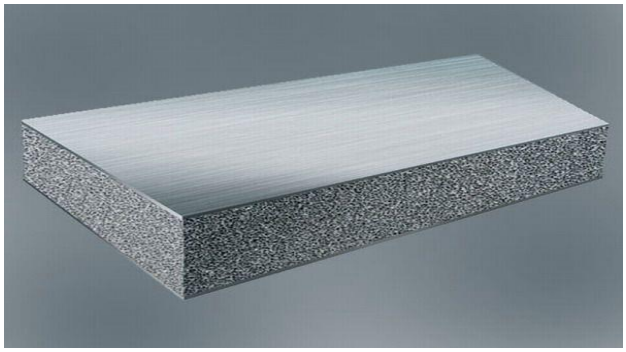

Fig 6 – Aluminium foam sandwich

1.5 Composition and Graphene reinforcement

We use Aluminium LM13 alloy which has a constant 3% wt. Boron Carbide (B4C) is prepared through stir casting. $CaCO_3$ is used as foaming in agent and as there is an increase in percentage of foaming agent, more gas bubbles are formed which increases porosity, which in turn decreases the density.

Boron Carbide (B4C) – As we know that metal properties can be enhanced only by alloying, the choice of alloying element plays a key role in improving the metal's required properties. Using boron carbide as reinforcement concludes that mechanical properties like tensile strength, impact strength, impact strength and tribological properties like wear resistance of composite are improved.

Fig 7: Stress v/s Strain graph at different strain rates

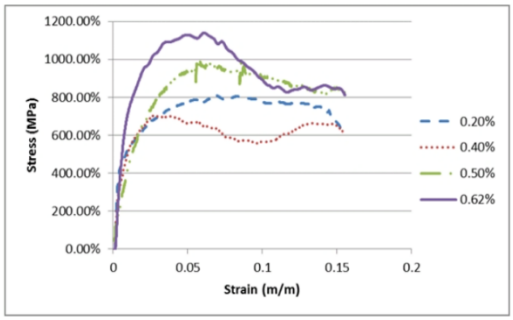

Figure 3.2 High strain rate (1000 s^{-1}) compressive stress-strain response for different graphene composition

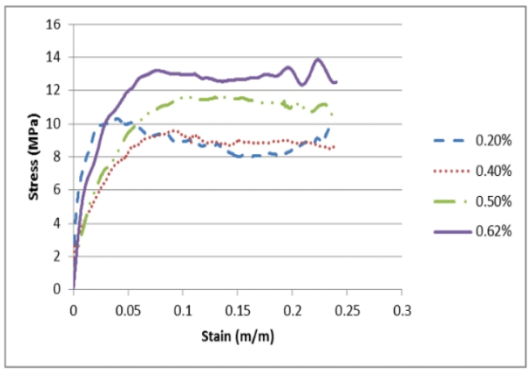

Figure 3.3 High strain rate (1400 s^{-1}) compressive stress-strain response for different graphene composition

Furthermore, the foam consists of 0.5%wt graphene nano-particle reinforcement and is prepared through the “Gas release in the melt” technique, using CaCO3 as the foaming agent. The varying composition of graphene has been studied, which gives varying results on the size of the plateau region during an impact, which was maximum for 0.62 % wt. in contrast, showing minimum results for 0.4 % wt. of graphene. However, a graphene-added hybrid foam consistently exhibits better energy absorption and plateau stress than one without graphene. Observing the two curves above, we can say that graphene reinforced aluminium foam clearly absorbs impact better than that of without graphene and also that it increases plateau region for impact absorption, thus increasing the time of impact.

1.6 Energy Absorption Behavior

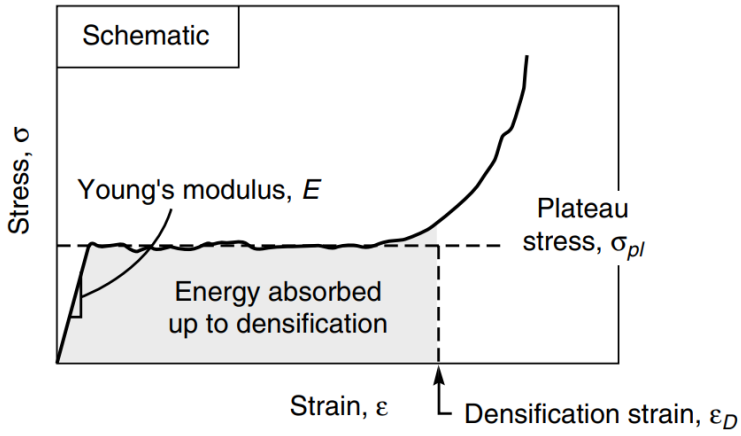

Fig 8: Stress v/s Strain graph

- The energy absorbing property of a material is defined as amount of energy that a material can absorb before it undergoes failure. On a stress-strain curve, the area under the curve gives a material's energy absorption capacity. When comparing the stress-strain curve of a metal with its metal foam, it is observed that metal foams energy absorption property is very high because of a bigger plateau region during an impact. Metal foam are materials with pores filled with gas and metal as a matrix. This enhances the mechanical properties of a material such as reduction in density, increase in toughness, low thermal conductivity and high energy absorption capacity. Automobiles, structures and aircrafts being reinforced with aluminum alloy foam, can reduce weight of structure to and absorb maximum amount of energy released during blasts. This makes it best suitable for defense applications and also the cellular structure

of aluminum foam makes it feasible to replace damaged bones. The below figure represents general trend of a stress-strain curve of aluminum foam under compression.

1.7 Compressive stress-strain curve for an ideal foam

The first region refers to collapse stress, whereas total deformation energy is absorbed in constant stress value for the plateau region. The final part is the densification region related to increasing stress at constant strain value. In this region, the cell walls are in close contact with each other.

Figure 9: Curve for Metal Foam Under Compression

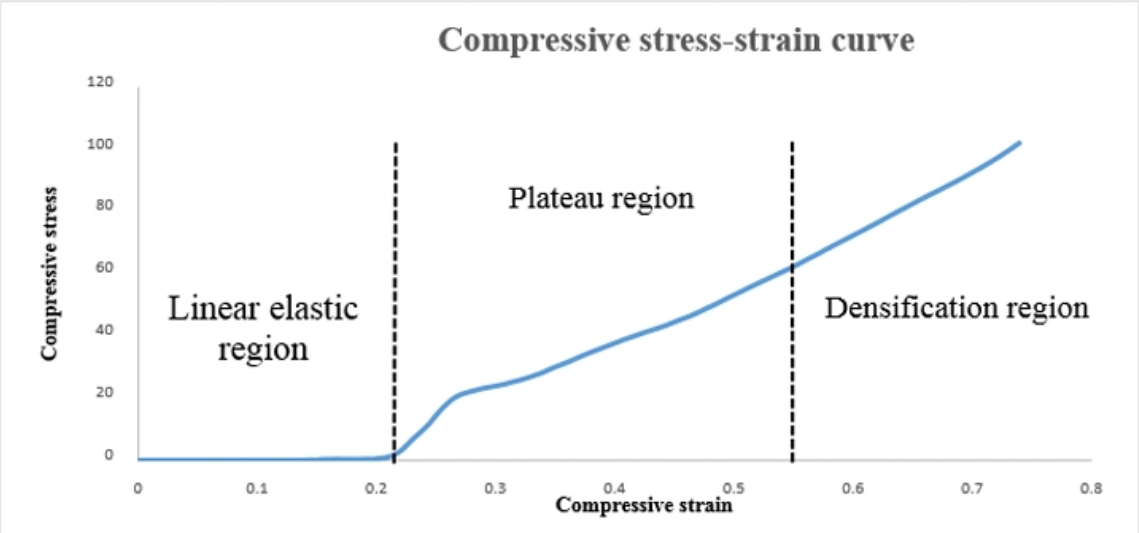

1.8 Uniaxial compression test

A typical uniaxial compression stress-strain curve for an aluminium foam is shown. The slope of the initial loading portion of the curve is lower than that of the unloading curve. Surface

strain measurements indicate that there is localized plasticity in the specimen at stresses well below the compressive strength of the foam, reducing the slope of the loading curve

Fig 10: Stress v/s Strain graph under Uniaxial Compression

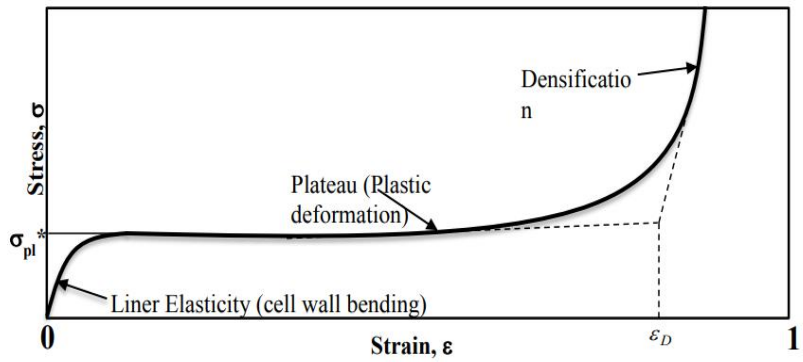

1.9 Stress-Strain Curve of Aluminium Foam and Aluminium rod

Fig 11: Stress-Strain curves for Aluminium Foam

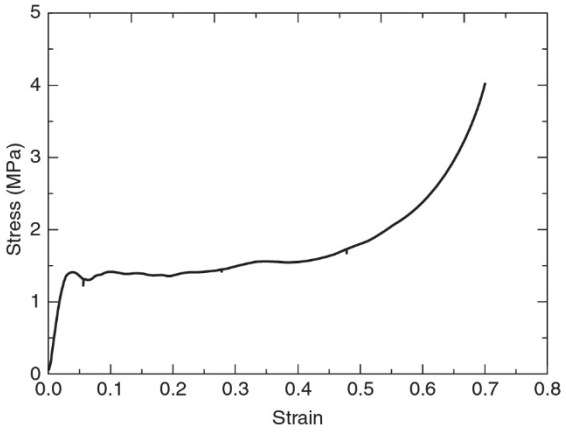

Fig 12: Stress-Strain curves for (a) pure aluminium

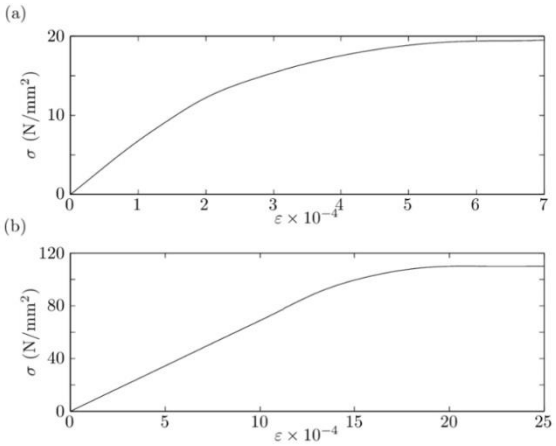

and (b) aluminium alloy

2. Theoretical Analysis

2.1 Introduction

The analytical solution for impact on composite material target made of laminated woven fibers based on matrix is presented. Therefore, the analysis of material properties for unidirectional laminates is used to develop material properties of woven fiber composite. Types of observed energies due to impact are developed and evaluated

2.2Unidirectional lamina

Analysis of the composite cylinder assemblage (CCA)[2] gives closed form results for the effective properties E_{11}, v_{12} and G_{12} and closed bounds for properties E_{22} and v_{21} and for the assumptions of transfers of isotropic fibers and isotropic matrix, a

Fig 13: Composite fiber lamina

$$E_{11} = E_m V_m + E_f V_f \qquad \ldots\ldots 2.1$$

$$\upsilon_{12} = \upsilon_m V_m + \upsilon_f V_f \qquad \ldots\ldots 2.2$$

$$G_{12} = G_m \left(\frac{V_f}{1/(G_f - G_m) + V_m/2G_m} \right) \qquad \ldots\ldots 2.3$$

$$E_{22} = \frac{E_m E_f}{E_m V_f + E_f V_m} \qquad \ldots\ldots 2.4$$

$$v_{21} = \frac{E_{11}}{E_{22}} v_{12} \qquad \ldots\ldots 2.5$$

For angled ply :-

$$E_{xx} = \left[\frac{m^4}{E_{11}} + \left(\frac{1}{G_{12}} - \frac{2v_{12}}{E_{11}} \right) m^2 n^2 + \frac{n^4}{E_{22}} \right]^{-1} \qquad \ldots\ldots 2.6$$

$$E_{yy} = \left[\frac{n^4}{E_{11}} + \left(\frac{1}{G_{12}} - \frac{2v_{12}}{E_{11}} \right) m^2 n^2 + \frac{m^4}{E_{22}} \right]^{-1} \qquad \ldots\ldots 2.7$$

$$G_{xy} = \left[\frac{1}{G_{12}} + 4\left(\frac{1+2v_{12}}{E_{11}} + \frac{1}{E_{22}} - \frac{1}{G_{12}}\right)m^2n^2\right]^{-1}$$

$$v_{xy} = E_{xx}\left[\frac{v_{12}}{E_{11}} - \left(\frac{1+2v_{12}}{E_{11}} + \frac{1}{E_{22}} - \frac{1}{G_{12}}\right)m^2n^2\right]$$

2.3 Random oriented discontinuous fiber composite

For the same fiber aspect ratio and same volume fraction of that to determine the prosperities of unidirectional fiber composite the isotropic properties of the random oriented discontinuous fiber composite are given by

$$G = \{E_{11} + 2E_{22}\}/8$$

$$E = \{3E_{11} + 5E_{22}\}/8$$

For woven fibers of finite-end satin, the properties will be decreased due to fibers bent, assuming that there is a multiplication factor which when multiplied by the infinite-end satin woven fibers composite properties gives the properties of the woven fibers of finite-satin then

$$(E_{11})_w = (E_{22})_w = W_E(E_{11})_\infty = W_E\frac{\left\{\left(1+\frac{v_{21}}{v_{12}}\right)^2 - 4v_{21}^2\right\}}{2(1-v_{12}v_{12})\left(1+\frac{v_{21}}{v_{12}}\right)}E_{11}$$

2.4 Impact analysis

2.4.1 introduction

The research of impact of woven hybrid composites has been experimental and Numerical. In order to understand the mechanisms in the woven

hybrid composite under low, high and ballistic velocities for impact, and the energy transfer between the impactor and the composite, analytical models are needed.

2.4.2 Constitutive relations

A laminated composite plate of length a, breadth b and thickness h with n arbitrarily oriented layers is considered. The plate axes and the layer details are illustrated in Fig. 3-2.

Fig 14: laminated composite

The x–y plane coincides with the middle plane of the plate and the z-axis is oriented along the thickness direction. The displacements u, v and w at any point (x, y, z) in the laminate are given by

$$u(x,y,z) = u^0(x,y) + z\,\theta x(x,y)$$

$$v(x,y,z) = v^0(x,y) + z\theta y(x,y)$$

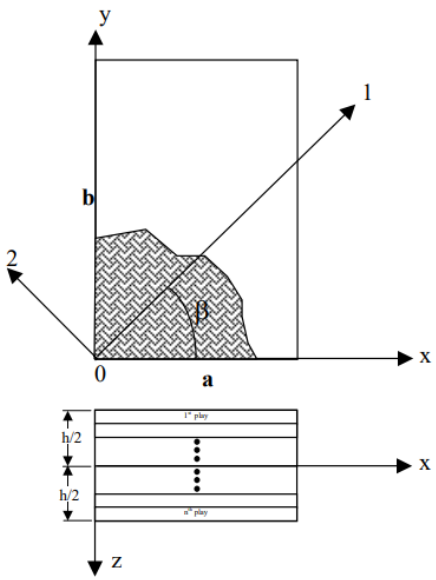

$$w(x,y,z) = w^0(x,y)$$

Where u^0 ,v^0 and w^0 denote the mid-plane displacements and θ_x and θ_y denote the rotations along the x and y axes, respectively. Considering first order

shear deformation, the strain components in a lamina are expressed as

$$\epsilon_x = \frac{\partial u}{\partial x} = \epsilon_x^0 + zk_x$$

$$\epsilon_y = \frac{\partial u}{\partial x} = \epsilon_y^0 + zk_y$$

$$\gamma_{xy} = \frac{\partial u}{\partial y} + \frac{\partial v}{\partial x} = \gamma_{xy}^0 + zk_{xy}$$

$$\gamma_{xy}^0 = \frac{\partial w}{\partial x} + \theta_x$$

$$\gamma_{yz}^0 = \frac{\partial \omega}{\partial y} + \theta_y$$

Where εx o , εy o and γxyo are mid-plane strains, kx, ky and kxy, are the plate curvatures and γxzo and γyzo are the transverse shear strains, respectively. The strains in the ith lamina at a distance z from the mid-plane in the matrix form are given by

$$\left[\varepsilon_x\ \varepsilon_y\ y_{xy}\ \gamma_{xz}\ \gamma_{yz}\right] = \left[\varepsilon_x^0\ \varepsilon_y^0\ \gamma_{xy}^0\ \gamma_{xz}^0\ \gamma_{y^2}^0\right] + z[kx\ k_y\ k_{xy}\ k_{xz}\ k_{yz}]$$

Here kxz and kyz are considered as zero. The stresses at any point in the kth lamina are

$$\{\sigma\} = \left[\underline{Q}_{ij}\right]_k \{\varepsilon\}$$

$$\{\sigma\} = [\sigma_x \sigma_y \sigma_z \tau_{xz} \tau_{yz} \tau_{\kappa y}]^T$$

2.5 Energy Balance

Based on the conservation of the total energy, the part of the kinetic energy of the projectile is absorbed by the plate, and assumed to be classified into four types which are: - 1- The strain energy due to dynamics of plate's theory (Contact energy) Uc . 2- Strain energy in the large deflection penetration zone ULd . 3- Delamination strain energy Udel. 4- Friction energy UF. The energy balance according to this classification for the impact becomes

$$\frac{1}{2} M_p v_{p_i}^2 = U_C + U_{LD} + U_{deL} + Uf + 1/2MV\text{^}2$$

Strain energy due to deformation of plate The equation of motion for the laminated composite plate subjected to dynamic load (impact) is

$$D_{11}\frac{\partial^4 w}{\partial x^4} + 2(D_{12} + D_{66})\frac{\partial^4 w}{\partial x^2 \partial y^2} + D_{22}\frac{\partial^4 w}{\partial y^4} + \rho h\frac{\partial^2 w}{\partial t^2} = q(x, y, t)$$

w(x,y) is the deflection along the z direction. q(x,y,t) is the intensity of transverse distributed load per unit area acting on the thin plate.D11, D16, D12, D66, D26, D22 are the flexural rigidity coefficients of the laminated plate. For especially orthotropic laminates (D16 = D26 =0), the governing differential equation becomes.

$$D_{11}\frac{\partial^4 w}{\partial x^4} + 2(D_{12} + D_{66})\frac{\partial^4 w}{\partial x^2 \partial y^2} + D_{22}\frac{\partial^4 w}{\partial y^4} + \rho h\frac{\partial^2 w}{\partial t^2} = q(x, y, t)$$

Friction energy :This observed energy is required to calculate the friction coefficient between the impactor and the plies. The friction process is very difficult due to delaminations, change in area of the contact, and load with time and thermal effect on the friction. Also after delaminations there are other losses in energies due to friction in delaminations of plies.

The friction coefficients between the composite and the projectile material are measured using friction disk with the details shown in the next chapter. The assumptions used in the friction work are that the friction is independent on the heat generation through the penetration.

This assumption is fair especially because the penetration time is very small to transfer heat through the surfaces. The Friction due to delamination is small with low movement compared with the friction due to penetration which vary clear in the geometry of the penetration and friction, and because the delamination energy was considered, then the friction through the delamination was considered through the analyses of the delamination. Then the analyses of frictional energy is based on
the variation of penetration loads through the
penetration.

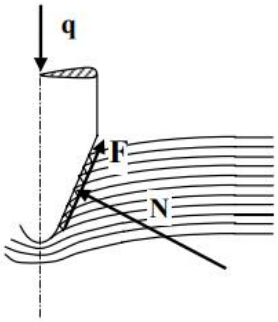

Fig 15: deformation occurring during impact

Using the momentum equation for the projectile

$$m(v_i - v_r) = \int \left(q - F\ cos\ cos\left(\frac{\emptyset}{2}\right) - \mu F\ sin\ sin\ (\emptyset\ /\ 2)\right) \cdot dt$$

3. MODELING USING ABAQUS

3.1 Impact Modeling Setup

The numerical modeling section employs ABAQUS CAE to simulate the dynamic interaction between a spherical-shaped steel projectile and a laminated composite carbon fiber plate. The laminated plates are arranged in [0/90] fiber orientation, representing a cross-ply configuration.

3.2 Material Properties

Laminated Sheets:

- Elasticity: The laminated sheets are modeled as elastic composite carbon fiber sheets.
- Density: The density is specified as 1600 kg/mm³.

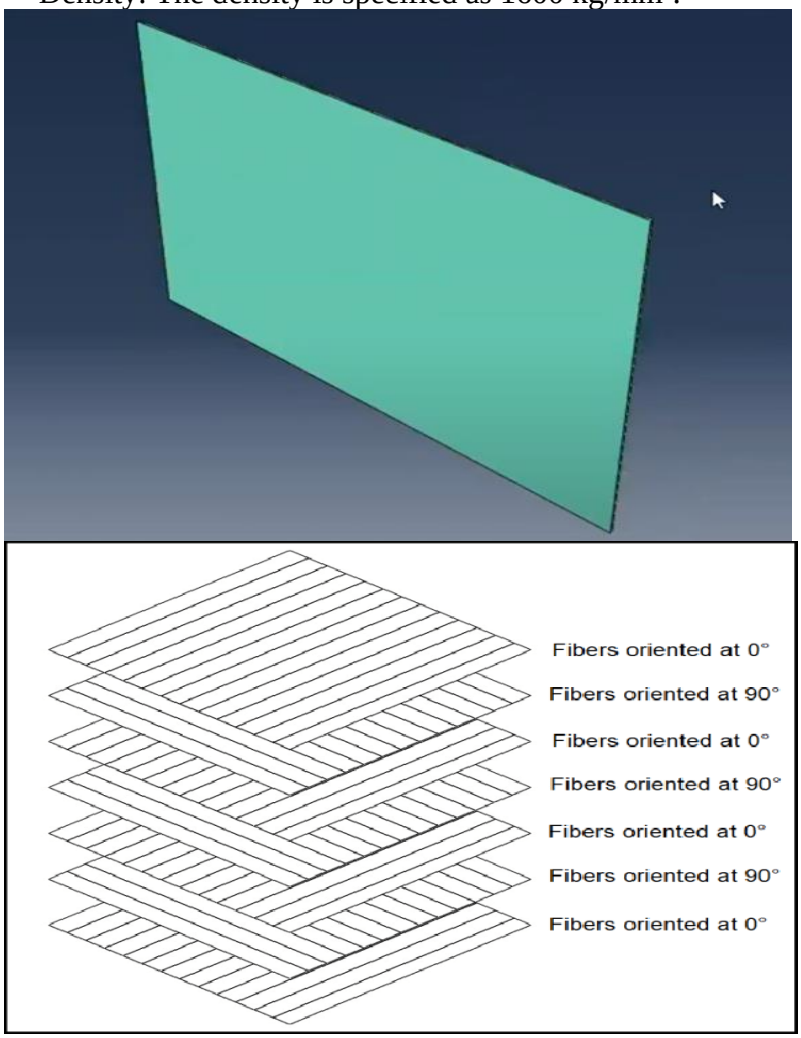

Fig 16: simulated model of the fiber plates and orientations

Impactor:

- Material: Steel. And the mass of the impactor being 3.2 kg.
- Density: The density of the steel impactor is specified.
- Isotropic Properties: The impactor is described as isotropic.

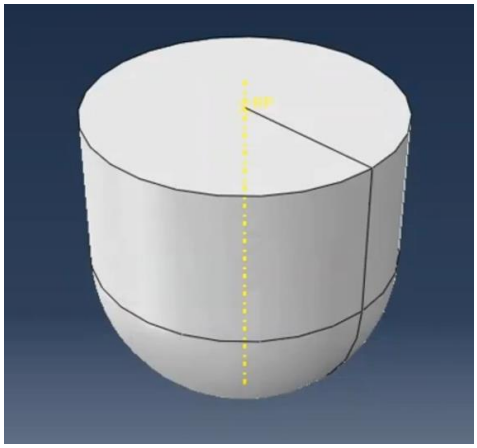

Fig 17: Impactor model

3.3 Simulation Setup

Analysis Type:

- Dynamic Explicit Analysis: This analysis type is chosen for its suitability in capturing high-speed impact scenarios.

- Progressive Damage Model: The Hashine damage model is implemented to simulate progressive damage accumulation.

-The Hashine damage model is a progressive damage model, meaning it allows for the gradual initiation and propagation of damage within a material as it undergoes loading. This is particularly important in impact scenarios, where materials experience dynamic and often complex loading conditions, therefore useful to our situations.

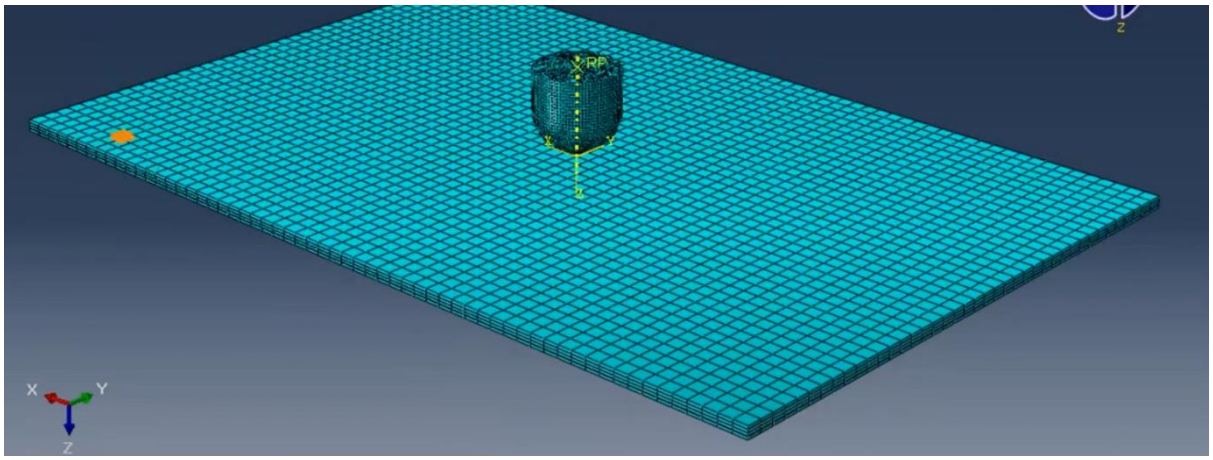

Fig 18: meshing of the impactor and plate

Interaction Module:

- Normal Behavior: Default hard contact behavior is employed.
- Tangential Behavior: Default tangential behavior with a penalty friction coefficient of 0.3 is implemented.
-In global seed we chose hex shaped elements and a mesh size of 2.5mm and explicit continuum shell for both the sheets and the impactor.

Boundary Conditions:

- The laminated plates are pinned at the ends, representing a fixed support condition.
- The projectile moves in the z-direction with an initial velocity of 2.5 m/s.

Meshing:

- Global Seed: Hexahedral (hex) shaped elements are chosen with a mesh size of 2.5 mm.
- Explicit Continuum Shell Elements: These elements are selected for both the laminated sheets and the impactor

3.4 Results and Post-Processing

- Force Peaks During Impact: The force-time graph exhibits peaks at the moments of impact, representing the maximum forces experienced during the interaction between the steel projectile and the laminated composite carbon fiber plate.

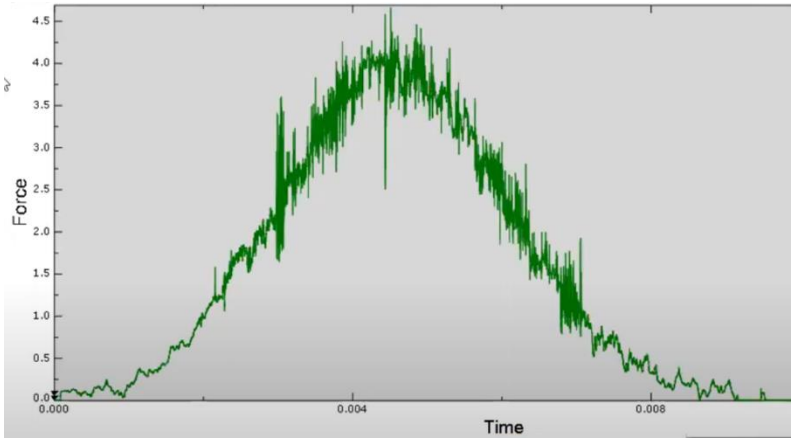

Fig 19: force vs time graph during impact

- Force Distribution on the Surface: Post-impact, the key observation is that after the impact, the force is dispersed evenly across the entire surface of the laminated plates. This means that the force is spread out uniformly rather than being concentrated in specific areas. The even distribution of force suggests that the stress, which is force per unit area, is uniform across the surface of the laminated plates

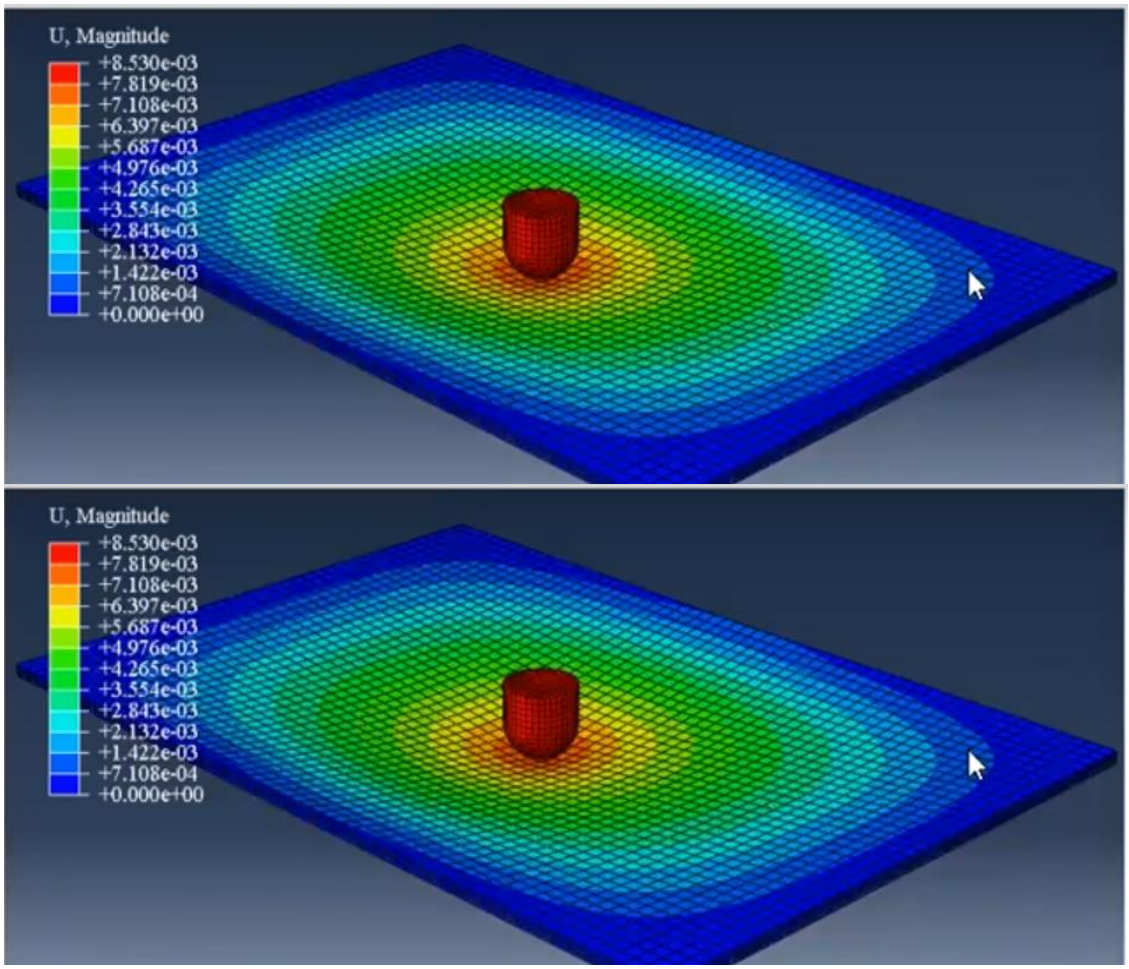

Fig 20: final model during impact

- Projectile Velocity Decay: After the initial impact, the velocity of the projectile decreases with time, signifying the transfer of energy to the laminated plates.
- Immediately upon contact with the target, the impactor experiences rapid deceleration. This deceleration is a result of the transfer of kinetic energy to the target material, causing deformation and damage.

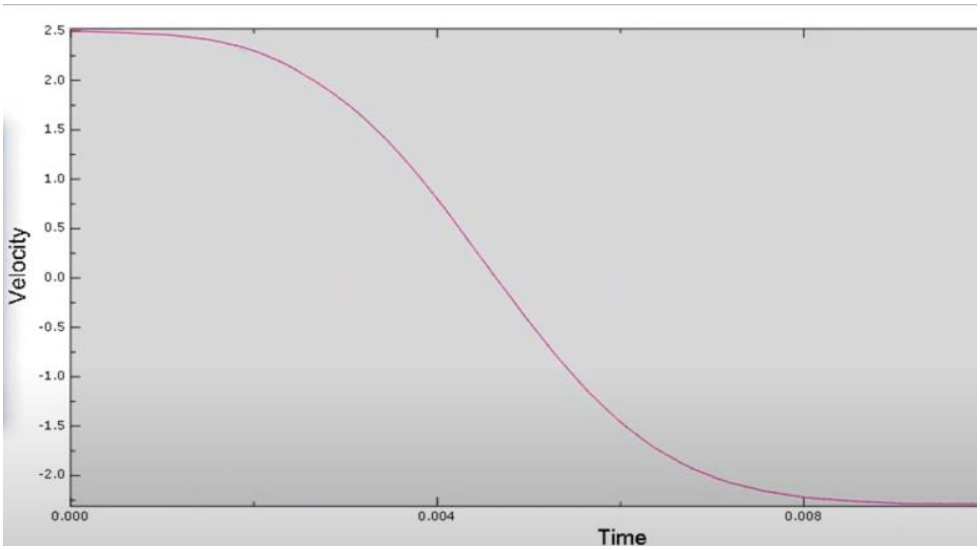

Fig 21: velocity vs time graph for the imapctor

- Following the initial impact and deceleration phase, the velocity of the impactor continues to decrease over time. This decay is a consequence of energy dissipation, plastic deformation, and other dynamic interactions between the impactor and the target material.

CONCLUSION AND FUTURE SCOPES

4.1 Conclusion

This phase of our BTP was mostly learning about the material properties, mechanisms and different compositional structures of Aluminum Foam and Also learning about the ABAQUS simulation software. As we started our research to come up with a viable solution, it leads us to dwell deep into the understanding of Lightweight energy absorbing materials, as material selection plays a vital role in meeting the functional requirements of components. Aluminium alloy foams are great energy absorbers and lightweight providing a wide range of potential applications. We learnt about aluminium foam sandwich and their different compositional and structural analysis. We came across various manufacturing methods for aluminium foam, and also did we learnt about the effect of boron carbide and graphene reinforcement in different percentages by weight composition and how it increased the compressive strength of the material. We then worked on the 3D simulation of carbon fibre composite models to find out the effect of impact on it through low velocity impactor. Also, we went through multiple research paper to understand the properties of aluminium foam and its impact behaviour. Finally, we compared the compressive stress-strain curve compressive behavior upon impact for an aluminum rod vs aluminum foam and also for different graphene composition under different strain rates.

References

An, Yukun, Siyi Yang, Hongyan Wu, Ertuan Zhao, and Zongshen Wang. 2017. "Investigating the Internal Structure and Mechanical Properties of Graphene Nanoflakes Enhanced Aluminum Foam." *Materials and Design* 134: 44–53. https://doi.org/10.1016/j.matdes.2017.08.031.

August, Anastasia, and B. Nestler. 2020. "About the Surface Area to Volume Relations of Open Cell Foam." *Engineering Research Express*, 0–13. https://iopscience.iop.org/article/10.1149/1945-7111/ab9a2c/meta.

Cernak, Ibolja, and Linda J. Noble-Haeusslein. 2010. "Traumatic Brain Injury: An Overview of Pathobiology with Emphasis on Military Populations." *Journal of Cerebral Blood Flow and Metabolism* 30 (2): 255–66. https://doi.org/10.1038/jcbfm.2009.203.

Dannemann, Kathryn A., and James Lankford. 2000. "High Strain Rate Compression of Closed-Cell Aluminum Foams." *Materials Science and Engineering A* 293 (1): 157–64. https://doi.org/10.1016/S0921-5093(00)01219-3.

Das, Sourav. 2017. "Graphene Reinforced Aluminum Foam for Automobile and Aerospace High Strain Rate Deformation of Gr-Al Metal Foam," no. August.

Davis, Harry J, and Herbert D Curchack. 1969. "Shock Tube Techniques and Instrumentation."

Dey, Chitralekha, Mahesh Thorat, Shiba N. Sahu, Kiran Akella, and Amol A. Gokhale. 2022. "Evaluation of Optimum Foam Density for Effective Design of Blast Absorbers." *Mechanics of Advanced Materials and Structures* 29 (3): 400–407. https://doi.org/10.1080/15376494.2020.1772416.

Downes, Stephen, Andy Knott, and Ian Robinson. 2015. "Towards a Shock Tube Method for the Dynamic Calibration of Pressure Sensors." *PTB - Mitteilungen Forschen Und Prufen* 125 (2): 24–37. https://doi.org/10.1098/rsta.2013.0299.

Epasto, Gabriella, Fabio Distefano, Linxia Gu, Hozhabr Mozafari, and Emanoil Linul. 2020.

Fleck, Norman. 2016. "Metal Foams : A Design Guide Metal Foams : A Design Guide" 3069 (FEBRUARY 2002): 264.

Golestanipour, M., A. Babakhani, and S. Mojtaba Zebarjad. 2020. "High-Velocity Perforation Behaviour of Sandwich Panels with Al/SiCp Composite Foam Core." *Journal of Composite Materials* 54 (11): 1483–95. https://doi.org/10.1177/0021998319883331.

Hou, Weihong, Feng Zhu, Guoxing Lu, and Dai Ning Fang. 2010. "Ballistic Impact Experiments of Metallic Sandwich Panels with Aluminium Foam Core." *International Journal of Impact Engineering* 37 (10): 1045–55. https://doi.org/10.1016/j.ijimpeng.2010.03.006.

Jing, Lin, Fei Yang, and Longmao Zhao. 2017. "Perforation Resistance of Sandwich Panels with Layered Gradient Metallic Foam Cores." *Composite Structures* 171: 217–26. https://doi.org/10.1016/j.compstruct.2017.02.097.

K., Lakshmi Chaitanya, and Srinivas Kolla. 2018. "A Review on Use of Aluminium Alloys in Automobile Components." *American International Journal of Research in Science, Technology, Engineering & Mathematics*, 103–7. https://doi.org/10.26634/jms.3.3.3673.

Saska, P., E. Krzystała, and A. Mężyk. 2011. "An Analysis of an Explosive Shock Wave

Impact onto Military Vehicles of Contemporary Warfare." *Journal of KONES* 18 (1): 515–24.

Solhi, Ayuob Mirzaei, Jafar Khalil Allafi, Mohammad Yusefi, Mojtaba Yazdani, and Ahad Mofammadzadeh. 2018. "Fabrication of Aluminum Foams by Using CaCO Foaming Agent," no. 2018: 1–27. https://doi.org/https://doi.org/10.1088/2053-1591/aad88a Manuscript.

Thorat, Mahesh, Shiba N. Sahu, Viren Menezes, and Amol A. Gokhale. 2022. "Back-Face-Signature-Monitored Evaluation of Foam-Sandwich Structures as Shock Mitigating Materials." *Journal of Materials Engineering and Performance*. https://doi.org/10.1007/s11665-022-06906-1.